Ab Initio Density Functional Theory Study of the Structure and Vibrational Spectra of Cyclohexanone and its Isotopomers

F. J. Devlin and P. J. Stephens*

Department of Chemistry, University of Southern California, Los Angeles, California 90089-0482

Received: August 4, 1998; In Final Form: November 11, 1998

We report ab initio density functional theory (DFT) calculations of the structure of cyclohexanone (**1**) in its chair conformation and of the unpolarized vibrational absorption (IR) spectra of four isotopomers of **1** (d_0, d_4, d_6, and d_{10}). DFT calculations use hybrid functionals, B3PW91 and B3LYP, and the TZ2P basis set. The results are compared to the electron diffraction (ED) structure of Dillen and Geise and liquid-phase IR spectra. Calculated and experimental structures are in reasonable agreement; however, the constraints imposed on the ED structure determination limit its accuracy. In the mid-IR (<2000 cm^{-1}), predicted vibrational spectra are in excellent agreement with experiment, permitting an essentially unambiguous assignment of all fundamentals; in the C−H and C−D stretching regions, agreement is worse due to anharmonicity/Fermi resonance and the spectra cannot be unambiguously assigned. Our assignments differ substantially from earlier assignments of Fuhrer et al., based on a constrained valence force field. Vibrational circular dichroism (VCD) spectra of d_1 and d_2 isotopomers have been reported for C−H and C−D stretching regions. Predicted spectra are in poor agreement with experiment, a result again attributable to anharmonicity.

We report a study of the structure and harmonic force field of cyclohexanone (**1**) using ab initio density functional theory (DFT). The structure of **1** was first determined experimentally in 1956 from electron diffraction data.[1] A chair conformation for the six-membered ring (Figure 1) was found. A structure having five independent parameters (three bond lengths and two bond angles) was fit to the data. A more recent study,[2] using electron diffraction and incorporating rotational constants from microwave spectroscopy, yielded a larger number of structural parameters of greater accuracy. However, to date a full structural study using either microwave spectroscopy or X-ray diffraction has not been reported. Thus, there has not been an unconstrained structure determination in which all independent internal coordinates have been obtained. A harmonic force field for **1** was developed by Fuhrer et al. in 1972.[3] Infrared (IR) and Raman spectra of **1** and three isotopomers, **1**-α,α,α′,α′-d_4 (**2**), **1**-β,β,β′,β′,γ,γ′-d_6 (**3**) and **1**-d_{10} (**4**), were obtained. An empirical, constrained valence force field (VFF) was refined using frequencies observed for all four isotopomers. Subsequently, this force field was used in the analysis of the IR absorption and vibrational circular dichroism (VCD) of the C−H and C−D stretching modes of the chiral **1**-α-d_1 (**5**) and **1**-trans-α,α′-d_2 (**6**) isotopomers.[4]

Ab initio DFT[5] has recently become a very powerful tool in the prediction of molecular structure, harmonic force fields, and vibrational frequencies and intensities. In our laboratories we have recently studied the structures, IR absorption, and VCD spectra of a range of organic molecules including 6,8-dioxabicyclo[3.2.1]octane[6] and several mono- and dimethyl derivatives,[7] camphor,[8] fenchone,[8] α-pinene,[9] and phenyloxirane.[10] Here, we use DFT to predict the structure and harmonic force field of the chair conformation of **1**, the fundamental vibrational frequencies and IR absorption intensities of **1**−**6**, and the VCD intensities of **5** and **6**. State-of-the-art hybrid density functionals,[11] B3PW91 and B3LYP,[12] are employed together with a large [5s4p2d/3s2p] basis set (TZ2P[13]). Our calculations are compared to the available experimental data and to new IR spectra for **1**. The vibrational spectra of **1**−**6** are reassigned.

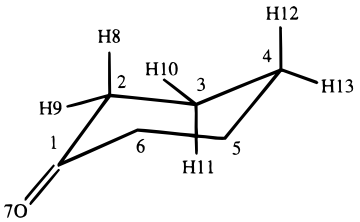

Figure 1. The chair conformation and atom numbering of **1**.

Methods

Cyclohexanone (**1**) was obtained from Aldrich and used without further purification; specified purity was 99.8%. FTIR spectra of CCl_4 and CS_2 solutions were obtained at 1 cm^{-1} resolution using a Nicolet MX-1 spectrometer.

The equilibrium geometry of **1** and the harmonic vibrational frequencies, dipole strengths, and rotational strengths of **1**−**6** were calculated using the ab initio DFT and HF/SCF methodologies via the GAUSSIAN program[14] as described previously.[6−10] The functionals B3PW91 and B3LYP[12] were used in DFT calculations. The basis sets TZ2P[13] and 6-31G*[15] were employed. Atomic axial tensors (AATs) were calculated using gauge-invariant atomic orbital (GIAO) basis sets.[5] All calculations used fully analytical derivative methods.[16]

The absorption spectrum of **1** was fit assuming Lorentzian band shapes in order to obtain experimental frequencies and dipole strengths, as described previously.[8,9]

Results

The structure of the chair conformation of **1** has been calculated using DFT, the TZ2P basis set, and the two functionals B3PW91 and B3LYP. The results are given in Table

* To whom correspondence should be addressed.

10.1021/jp983267h CCC: $18.00
Published on Web 01/28/1999

TABLE 1: Structural Parameters of 1[a]

	B3PW91[b]	B3LYP[b]	I[c]	II[d]
bond lengths				
C1−O7	1.209	1.211	1.24(2)	1.229(3)
C1−C2	1.514	1.518		1.503(4)
C2−C3	1.534	1.541	1.54(1)	1.542(2)
C3−C4	1.525	1.531		1.545[g]
C2−H8[e]	1.097	1.096		
C2−H9[f]	1.089	1.088		
C3−H10[f]	1.092	1.091		
C3−H11[e]	1.094	1.093	1.09(2)	1.088(2)
C4−H12[e]	1.095	1.094		
C4−H13[f]	1.092	1.091		
bond angles				
O7C1C2	122.4	122.3		
C6C1C2	115.2	115.3	117 (3.0)	115.3(0.3)
C1C2C3	111.9	112.0		111.5(0.1)
C2C3C4	111.6	111.7	109.5 (2.5)	110.8(0.2)
C3C4C5	111.1	111.2		
H8C2H9	107.7	107.7		
H10C3H11	106.5	106.5		106.0(0.9)
H12C4H13	106.5	106.6		
torsional angles[h]				
O7C1C2C3	131.4	131.8		128.3[i]
C6C1C2C3	48.7	48.4		51.7[i]
C1C2C3C4	51.8	51.5		53.0[i]
C2C3C4C5	56.3	56.2		56.3[i]

[a] Atom numbering as in Figure 1. Bond lengths and angles in angstroms and degrees, respectively. [b] DFT calculations using the TZ2P basis set. [c] From electron diffraction data (ref 1). Standard deviations in parentheses. [d] From electron diffraction and microwave spectroscopic data (ref 2). Standard deviations in parentheses. [e] Axial C−H bond. [f] Equatorial C−H bond. [g] Constrained relative to C2−C3. [h] Signs of torsional angles are omitted. [i] Not independent variables.

1, together with the results obtained from electron diffraction data. Structures I and II are the results of Romers[1] and Dillen and Geise,[2] respectively. Romers assumed that (i) all C−C bond lengths, (ii) all C−H bond lengths, (iii) CCC angles $C_1C_2C_3$, $C_2C_3C_4$, and $C_3C_4C_5$, and (iv) all HCH angles are equal. In the later study of Dillen and Geise, constraints i and iii were relaxed, allowing the C_1-C_2 bond length to differ from the bond length of C_2-C_3 and C_3-C_4 and the $C_1C_2C_3$ bond angle to differ from the bond angles of $C_2C_3C_4$ and $C_3C_4C_5$. In addition, it was assumed that the C_3-C_4 bond length is 0.003 Å greater than that of C_2-C_3.

The B3PW91 and B3LYP calculations give very similar structural parameters. Torsional angles, defining the conformation of the C_6O framework, agree within 0.4°. The $O_7C_1C_2C_6$ atoms are planar to within 0.1°. The C−C and C═O bond lengths agree within 0.007Å; B3LYP values are uniformly greater than B3PW91. CCC and OCC bond angles agree within 0.2°; B3LYP values are greater than B3PW91 except for $O_7C_1C_2$. C−H bond lengths agree within 0.001 Å; B3LYP values are uniformly smaller than B3PW91. HCH bond angles agree within 0.1°; B3LYP values are uniformly greater than B3PW91. Both calculations order C−C bond lengths: $C_2-C_3 > C_3-C_4 > C_1-C_2$ with a range of ∼0.02 Å. The CCC bond angles are similarly ordered: $C_6C_1C_2 > C_1C_2C_3 > C_2C_3C_4 > C_3C_4C_5$ with a range of ∼4°. Both calculations predict that equatorial C−H bond lengths are uniformly smaller than axial C−H bond lengths; the difference is 0.002−0.003 Å for bonds to C_3 and C_4 and 0.007 Å for bonds to C_2. All C_3−H and C_4−H bond lengths lie between the axial and equatorial C_2−H bond lengths. Both calculations predict that $H_8C_2H_9 > H_{12}C_4H_{13} > H_{10}C_3H_{11}$, with a range of ∼1.2°.

Overall, agreement between calculated and observed (structure II) parameters is quite good. The torsional angles are within 4°. The C−C and C═O bond lengths are within 0.02 Å. The CCC bond angles are within 1°. The C−H bond lengths are within 0.01 Å and the HCH bond angles are within 2°. The differences of the calculated parameters from experiment are substantially greater than the differences between the B3LYP and B3PW91 parameters. The ordering C_2-C_3, $C_3-C_4 > C_1-C_2$ is correctly predicted; however, the assumption that $C_3-C_4 > C_2-C_3$ made by Dillen and Geise is not supported by the calculations. The ordering $C_6C_1C_2 > C_1C_2C_3 > C_2C_3C_4$, $C_3C_4C_5$ is correctly predicted. The predicted orderings of $C_2C_3C_4$, $C_3C_4C_5$, of the C−H bond lengths and of the HCH bond angles cannot be compared to experiment due to the constraints imposed in the analysis of the experimental data.

DFT/TZ2P harmonic vibrational frequencies and dipole strengths for **1** have been calculated using B3PW91 and B3LYP; the results are given in Table 2. Unpolarized absorption spectra predicted thence for the mid-IR and C−H stretching spectral regions are shown in Figures 2 and 3, respectively. Experimental spectra of CCl_4 and CS_2 solutions of **1** have been measured at 1 cm^{-1} resolution. The spectra are extremely similar. The CCl_4 solution spectrum is shown in Figure 2, except in the region of strong CCl_4 absorption where the CS_2 spectrum is shown. The CS_2 spectrum is shown in Figure 3.

Assignment of the mid-IR spectrum using the DFT calculations is straightforward, as shown in Figure 2. The fundamentals 7, 8, 11−18, 21, 24, 27, 30, 31, and 34 are resolved and immediately assignable. The bands at 410, 748, 1118, 1311, 1347, and 1449 are assigned to unresolved pairs of modes, specifically 4/5, 9/10, 19/20, 25/26, 28/29, and 32/33. The fundamentals 22 and 23 are assigned to weak shoulders at 1227 and 1243 cm^{-1}. The fundamental 6 is not observed; it is either very weak or unresolved from mode 7.

The spectra predicted by the B3PW91 and B3LYP functionals are overall qualitatively very similar. Only for modes 13 and 14 are the predicted spectra in Figure 2 substantially different. B3PW91 predicts a very unequal distribution of intensities, modes 13 and 14 being weak and strong, respectively. Conversely, B3LYP predicts comparable intensities. Experimentally, mode 13 is significantly weaker than 14, but not by as much as predicted by B3PW91. In the case of the pairs of modes 19/20 and 28/29, the two functionals also predict quite different intensity ratios. Since these modes are unresolved experimentally, we cannot assess the relative accuracies of the predictions.

To assess the quantitative accuracies of the mid-IR frequencies and dipole strengths of **1** predicted by the DFT/TZ2P calculations we have obtained experimental values for these parameters by Lorentzian fitting. The fit is shown in Figure 2. The frequencies, dipole strengths, and bandwidths obtained are given in Table 2. Calculated and experimental frequencies and dipole strengths are compared in Figures 4 and 5. With the exception of mode 4, calculated frequencies are higher than experiment. The percentage errors lie within the range 0−4%. In the case of B3PW91 the errors vary fairly monotonically with frequency, increasing with increasing frequency. In the case of B3LYP, the variation is significantly less regular, indicating that the relative spacing of modes is less accurately predicted. A significant fraction of the errors in calculated frequencies can be attributed to the contribution of anharmonicity to the experimental frequencies.[17] Calculated and experimental dipole strengths are in comparable agreement for the two functionals. The largest discrepancy is for the band at 490 cm^{-1}, assigned to mode 7, whose intensity is significantly underestimated. Note that in the case of bands to which two, unresolved fundamentals are assigned Lorentzian fitting was carried out assuming a single

TABLE 2: Cyclohexanone-d_0 (1)[a]

DFT/TZ2P						this work[c]					
		B3LYP		B3PW91		CCl_4			ref 3		
mode	symmetry[b]	ν	D	ν	D	ν	D	γ	ν [e]	symmetry	mode [f]
45	A′	3099	13.8	3113	12.8	2960			2961 s*	A′	45
44	A″	3098	21.6	3112	19.6					A″	44
										A′	43
43	A′	3067	53.4	3082	48.6						
42	A″	3063	37.9	3077	33.1	2940			2940 vs	A″	42
41	A′	3060	50.2	3074	43.2						
									2920 s*	A′	41
										A′	40
									2894 s	A″	39
40	A′	3024	44.8	3033	41.9	2866			2867 s	A′	38
39	A″	3022	21.9	3033	23.9					A″	37
38	A′	3011	15.3	3022	14.0	2859			2859 s*	A′	36
37	A′	3009	12.2	3020	15.1						
36	A″	3004	1.4	3016	1.4						
35	A′	1777	509.7	1795	511.0	1716	558.4	6.0	1718 vvs	A′	35
34	A′	1513	5.4	1503	6.0	1463	8.8	3.6	1462 m	A′	34
33	A″	1499	15.0	1488	18.3	1449	53.1	3.4	1449 vs	A″	33
32	A′	1498	26.5	1487	30.7					A′	32
31	A′	1476	24.8	1465	27.7	1429	32.3	4.9	1429 s	A″	31√
30	A″	1468	23.3	1456	26.2	1420	28.5	5.1	1421 s	A′	30√
										A″	29√
29	A″ (A′)	1384	8.6	1379	5.3	1347	22.3	3.2	1346 s	A′	28
28	A′ (A″)	1382	1.9	1376	7.3						
27	A″	1374	10.9	1366	15.4	1337	16.7	2.6	1338 s	A″	27
26	A′	1348	14.0	1342	15.2	1311	64.3	4.5	1311 vs	A″	26√
25	A″	1338	36.5	1337	49.3					A′	25√
24	A″	1295	4.3	1290	5.0	1264	6.3	3.5	1263 m	A″	24
23	A′	1277	0.5	1275	0.5	1243	1.6	6.4	1247 m*	A′	23
										A″	22√
22	A′	1254	3.3	1247	3.2	1227	12.9	7.1			
21	A″	1246	86.1	1243	79.0	1221	70.6	4.1	1220 vs	A′	21√
									1185 w*	A″	20√
20	A″ (A′)	1141	1.3	1140	68.1	1118	71.7	4.3	1117 vs	A′	19
19	A′ (A″)	1134	73.5	1135	1.4						
18	A″	1079	2.4	1089	4.2	1072	5.6	5.0	1072 w	A″	18
17	A″	1066	30.2	1061	23.3	1051	23.2	4.7	1049 m	A″	17
16	A′	1027	12.6	1032	12.3	1018	12.6	2.7	1018 m	A′	16
15	A′	1000	6.4	1004	6.0	991	4.3	2.4	990 w	A′	15
14	A″	919	13.7	918	30.2	908	24.7	2.8	907 s	A″	14
13	A″	895	16.1	900	2.6	894	15.2	6.1	894 m	A″	13
12	A′	878	19.8	872	23.0	863	19.5	2.6	861 m	A′	12
11	A′	838	1.1	849	1.6	837[d]	2.2	3.7	838 vw	A′	11
10	A″	762	29.5	757	27.6	748[d]	45.4	4.8	748 s	A″	10
9	A′	748	25.8	755	23.6					A′	9
8	A′	656	10.9	658	12.1	652	23.7	7.6	652 m	A′	8
7	A″	494	72.5	493	73.4	490	122.5	7.7	490 s	A′	7√
										A″	6√
6	A′	479	2.8	473	3.4						
									460 vw	A″	5√
5	A″	418	21.9	413	22.0	410	53.6	5.0	410 m	A′	4
4	A′	405	15.1	403	14.6						
3	A′	305	3.6	303	3.5				315	A′	3
2	A″	178	19.3	175	20.5				190	A″	2
1	A′	91	166.7	89	160.8				112	A′	1

[a] Frequencies, ν, in cm^{-1}; dipole strengths, D, in 10^{-40} esu^2 cm^2; bandwidths, γ, in cm^{-1}. [b] B3PW91 symmetry; symmetry for B3LYP in parentheses. [c] From Lorentzian fitting except for C−H stretching modes where peak frequencies are given. [d] Measured in 0.95 M CS_2 solution at 1 cm^{-1} resolution. [e] IR frequencies of neat liquid **1**; an asterisk denotes an inflection. s = strong, vs = very strong, vvs = very very strong, m = medium. [f] Mode assignments from ref 3 differing from those deriving from the DFT calculations are checked (√).

band. For these bands, in Figure 5, the experimental dipole strength is compared to the sum of the calculated dipole strengths of the two modes.

Assignment of the C═O stretching mode, 35, is straightforward. The assignment of the C−H stretching modes (36−45) is more difficult. Comparison of the predicted and experimental spectra (Figure 3) suggests assignment of the peaks at 2960, 2940, 2866, and 2859 to modes 44/45, 41−43, 39/40, and 37/38, respectively. This leaves additional peaks at 2894 and <2850 cm^{-1} unassigned. An alternative, and quite likely, possibility is that the peak at 2894 cm^{-1} is attributable to one of the fundamentals 37−40, shifted to higher frequency by Fermi resonance. In view of the complexity of this spectral region, we have not attempted Lorentzian deconvolution.

Assignment of the fundamentals of **1** was previously reported by Fuhrer et al., based on IR and Raman spectra.[3] Their IR spectrum (ref 3, Figure 5A) of **1** in CCl_4 and CS_2 agrees well with our spectrum in Figures 2 and 3. Their IR frequencies (for neat liquid **1**) and assignments are also given in Table 2. The experimental frequencies are very close to those obtained in

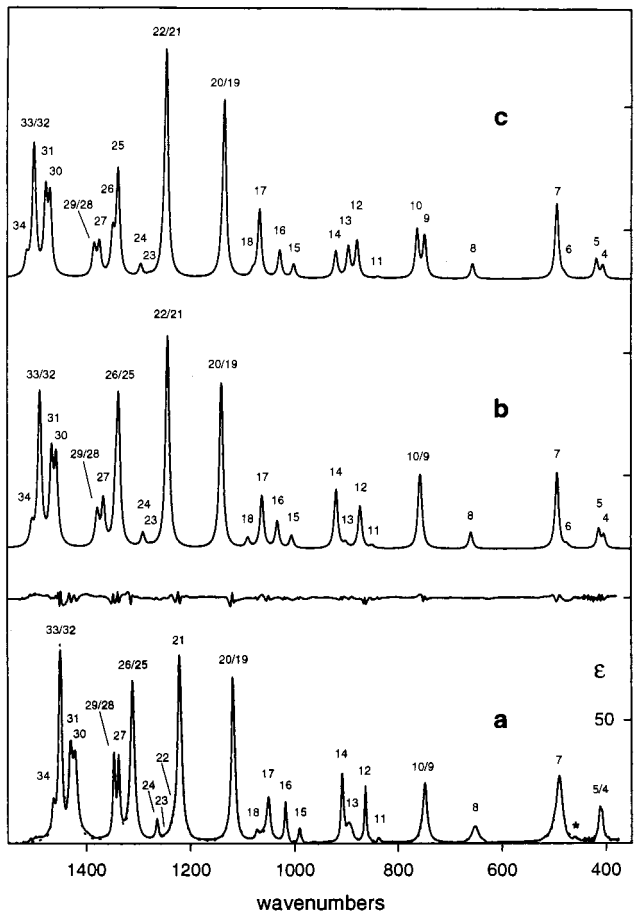

Figure 2. Mid-IR absorption spectra of **1**: (a) experimental spectrum, (b) calculated spectrum (B3PW91/TZ2P), (c) calculated spectrum (B3LYP/TZ2P). The solid line spectrum in a is for CCl_4 (0.96 M, 1597−850 cm^{-1}, 700−375 cm^{-1}) and CS_2 (0.95 M, 850−700 cm^{-1}) solutions of **1**. The dotted line spectrum is a Lorentzian fit. The difference spectrum (experiment−fit) is plotted above. The asterisked band at ∼460 cm^{-1} is not due to **1**. The calculated spectra in b and c use Lorentzian band shapes, $\gamma = 4.0$ cm^{-1}. Fundamentals are numbered.

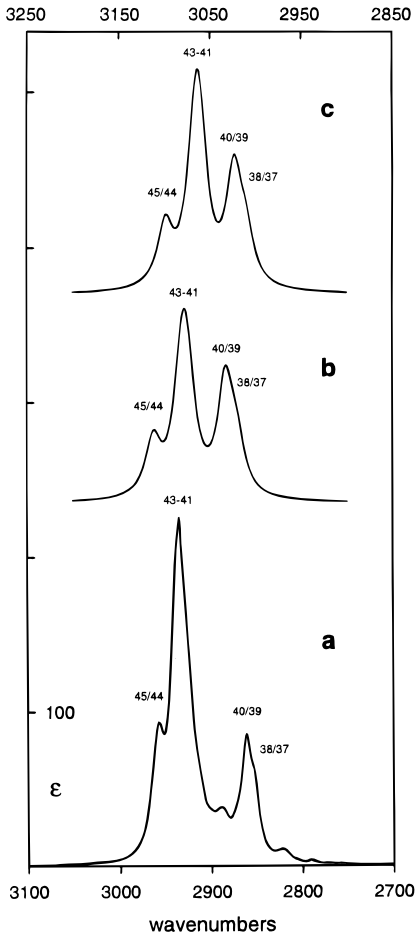

Figure 3. C−H stretching absorption spectra of **1**: (a) experimental spectrum (0.95 M solution in CS_2), (b) calculated spectrum (B3PW91/TZ2P), (c) calculated spectrum (B3LYP/TZ2P). Calculated spectra use Lorentzian band shapes with $\gamma = 10.0$ cm^{-1}. Fundamentals are numbered. Upper frequency scale applies to b and c.

this work. Fuhrer et al. did not report a band at 1227 cm^{-1}, but did find bands at 1185 and 460 cm^{-1} not observed in this work. The earlier assignments of Fuhrer et al. differ from those of this work as follows: (1) the 460 and 1185 cm^{-1} bands are assigned as fundamentals (5 and 20); (2) the 410 cm^{-1} band is assigned to mode 4 alone; (3) both modes 6 and 7 are assigned to the 490 cm^{-1} band; their symmetries are reversed; (4) mode 19, but not mode 20, is assigned to the 1118 cm^{-1} band; (5) the band at 1221 cm^{-1} is assigned as A′, not A″; (6) modes 22 and 23, of A″ and A′ symmetries respectively, are assigned to the 1243 cm^{-1} band; (7) the symmetries of modes 25 and 26, assigned to the 1311 cm^{-1} band, are reversed; (8) mode 28 (A′) is assigned to the 1347 cm^{-1} band, but mode 29 (A″) is not assigned; (9) the symmetries of modes 30 and 31, assigned to the 1420 and 1429 cm^{-1} bands, are reversed; (10) with the exception of modes 42, 44, and 45, C−H stretching modes are assigned differently. Our work thus substantially revises the earlier assignment of Fuhrer et al.

Fuhrer et al. also assigned far-IR absorption at 112, 190, and 315 cm^{-1} to modes 1, 2, and 3, respectively. Gas-phase studies by Carreira and Lord[18] and by Smithson et al.[19] led to frequencies of 92, 182, and 308 cm^{-1} for modes 1, 2, and 3. Our DFT/TZ2P frequencies are in excellent agreement with these data. Predicted relative intensities are also in good qualitative agreement with experiment (ref 19, Figure 1).

Fuhrer et al. also reported IR and Raman spectra of d_4, d_6, and d_{10} isotopomers of **1: 2**, **3**, and **4**. In **2**, the four α-H of **1** are substituted by D; in **3**, the four α-D of **4** are substituted by H. IR frequencies reported by Fuhrer et al. are given in Tables 3−5. DFT/TZ2P fundamental frequencies and dipole strengths predicted using B3PW91 and B3LYP are also given in Tables 3−5. The mid-IR spectra predicted thence for B3PW91 are shown in Figure 6; the C−H and C−D stretching spectra are shown in Figure 7.

Comparison of the B3PW91 spectrum for **2** (Figures 6 and 7) to the reported spectrum (ref 3, Figure 5B) and of the B3PW91 and experimental frequencies (Table 3) leads to the assignment detailed in Table 3. Fundamentals 1−5, 7−11, 13−26, 34, and 35 are resolved. Modes 6, 12, and 31 are predicted to be very weak and are not observed. The pairs of modes 27/28, 29/30, and 32/33 are not resolved. Modes 36−39 are responsible for absorption in the range 2000−2300 cm^{-1}. However, more than four peaks are observed and the assignment of the spectrum is undoubtedly complicated by Fermi resonance. Modes 40−45 are responsible for absorption in the range 2800−3000 cm^{-1}. Experimentally, there are two, somewhat structured peaks at 2942 and 2868 cm^{-1}. We tentatively assign the higher peak to modes 43−45 and the lower peak to modes 40−42. Support for the assignment of the mid-IR modes 4−34 is provided by the comparison of B3PW91 and experimental frequencies shown in Figure 4. Percentage errors lie within the same range and show the same variation with frequency as was

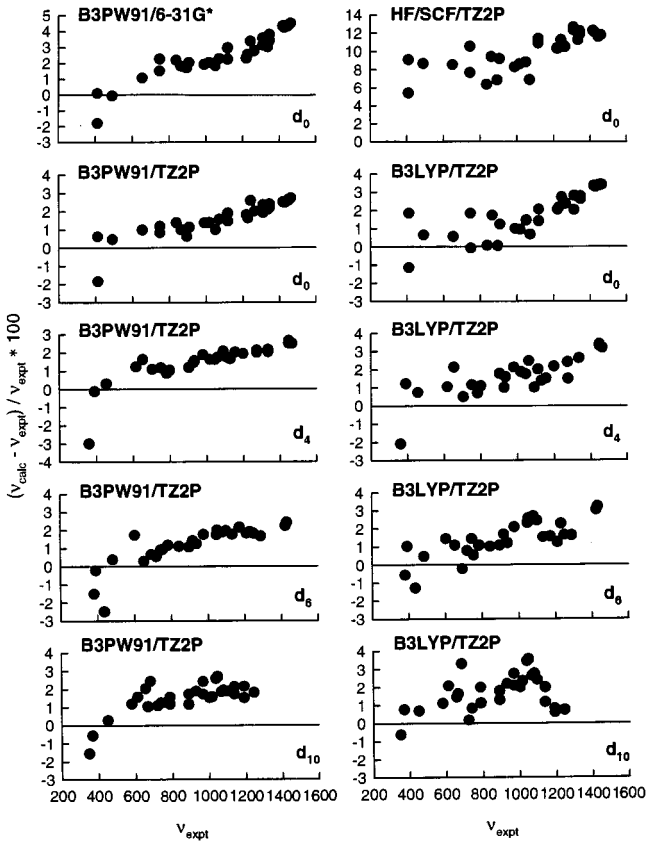

Figure 4. Comparison of calculated and experimental frequencies for **1**−**4**. Frequencies in cm^{-1}.

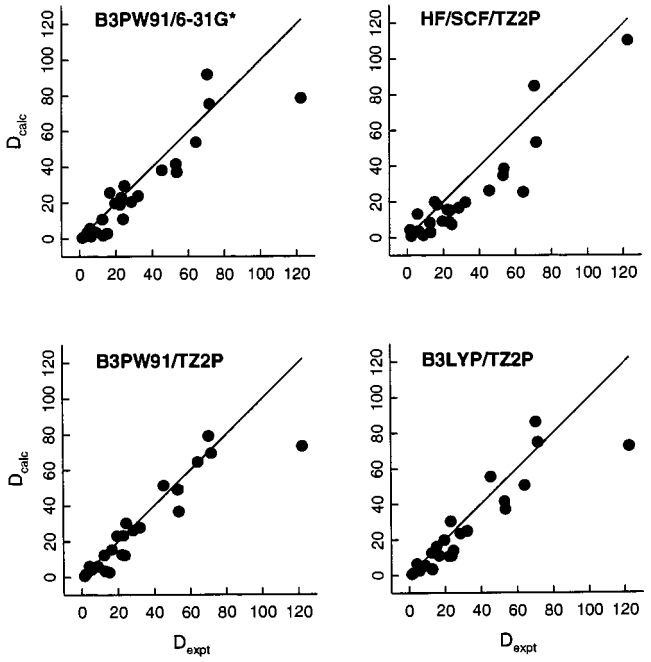

Figure 5. Comparison of calculated and experimental dipole strengths for **1**. Dipole strengths in 10^{-40} esu^2 cm^2.

found for the mid-IR modes 4−34 of **1** (Figure 4). Note that the very weak absorption at 1374 cm^{-1} reported by Fuhrer et al. is not assigned by us to mode 31 because this assignment would not be consistent with the expected ∼2% error in the calculated frequency.

The B3LYP frequencies and dipole strengths (Table 3) and spectrum for **2** are very similar to those predicted by B3PW91 and lead to an identical assignment. B3LYP and experimental frequencies for modes 4−34 are compared in Figure 4. As with **1** the variation in percentage error with frequency is somewhat less regular than with B3PW91.

The assignment reported by Fuhrer et al. is also given in Table 3. As for **1**, their assignment is substantially different from that resulting from the DFT calculations. Differences are indicated in Table 3.

Comparison of the B3PW91 spectrum for **3** (Figures 6 and 7) to the reported spectrum (ref 3, Figure 5C) and the B3PW91 and experimental frequencies (Table 4) leads to the assignment detailed in Table 4. The fundamentals 1−15, 17−24, 26−31, and 33−35 are resolved. Modes 25 and 32 are predicted to be very weak and are not observed. Mode 16 is also predicted to be very weak, but to be very close in frequency to mode 17, whose predicted intensity is much greater. The C−D stretching modes 36−38 and 39−41 can be most simply assigned to the two structured bands at 2110 and 2209 cm^{-1} respectively. The assignment of the C−H stretching modes is less straightforward since the observed spectrum is more complex than the predicted spectrum (Figure 7). The simplest option is to assign modes 42/43 and 44/45 to the bands at 2900 and 2965 cm^{-1}, the absorption at <2900 cm^{-1} being due to overtone/combination bands. Fermi resonance is quite likely to exist, however, rendering this assignment simplistic.

The B3LYP functional leads to very similar predictions. Only in the case of modes 16 and 17 is there a qualitative difference from B3PW91, the ordering of the A′ and A″ modes being reversed. B3LYP would assign the 897 cm^{-1} band to mode 16 instead of 17.

Comparison of calculated B3PW91 and B3LYP frequencies to experiment is shown in Figure 4. The accuracies of the calculated frequencies are very similar to those for **1** and **2**, supporting our assignment. Again, the errors in B3LYP frequencies are less regular than the errors in B3PW91 frequencies.

As with **1** and **2**, our assignment for **3** differs substantially from that of Fuhrer et al. (Table 4).

Comparison of the B3PW91 spectrum for **4** (Figures 6 and 7) to the reported spectrum (ref 3, Figure 5D) and of the B3PW91 and experimental frequencies (Table 5) leads to the assignment detailed in Table 5. The fundamentals 1−5, 7−14, 20, 23−29, 34, and 35 are resolved. Modes 6 and 15 are predicted to be very weak and are not observed. The pairs of modes 16/17, 18/19, 21/22, 30/31, and 32/33 are not resolved. The C−D stretching spectrum (ref 3, Figure 5D) is more complex than the predicted spectrum (Figure 7). We tentatively assign the band at 2111 cm^{-1} to modes 36−40, the band at 2210 cm^{-1} to modes 41−43 and the shoulder at 2221 cm^{-1} to modes 44/45.

The B3LYP functional leads to very similar predictions and an identical assignment.

Comparison of B3PW91 and B3LYP frequencies to experiment for modes 4−34 is shown in Figure 4. The accuracies of the calculated frequencies are very similar to those for **1**−**3**, supporting our assignment.

As with **1**−**3**, our assignment for **4** differs substantially from that of Fuhrer et al. (Table 5).

DFT/B3PW91/TZ2P vibrational frequencies, dipole strengths and rotational strengths have been calculated for the d_1- and trans-d_2 isotopomers of **1** (**5** and **6**) in which α-H atoms are substituted by D. The results are given in Tables 6 and 7 for the C−H and C−D stretching modes. Absorption and VCD spectra predicted thence are given in Figures 8 and 9. Experimental absorption and VCD spectra were reported by Nafie and

TABLE 3: Cyclohexanone-d_4 (2)[a]

		DFT/TZ2P						
		B3LYP		B3PW91		ref 3		
mode	symmetry	ν	D	ν	D	ν[b]	symmetry	mode[d]
45	A′	3066	48.6	3081	45.3	2942 vs	A′	45
44	A″	3062	35.6	3077	30.4		A″	44
43	A′	3060	51.0	3074	44.5	2909 vs*	A′	43
42	A′	3024	36.0	3033	33.0	2868 vs	A′	42
41	A″	3022	26.3	3032	28.4		A″	41
40	A′	3010	16.8	3021	19.3	2858 s*	A′	40
39	A′	2294	9.5	2304	8.3	2229 s	A′	39
38	A″	2291	8.9	2301	8.2	2217 m*	A″	38
37	A′	2196	17.6	2204	16.2	2147 m	A′	37
36	A″	2190	0.6	2199	0.4	2110 m	A″	36
35	A′	1771	516.7	1789	517.1	1710 vvs	A′	35
34	A′	1512	10.4	1502	11.8	1465 s	A′	34
33	A″	1498	12.1	1487	14.4	1449 vs	A′	33√
32	A′	1497	19.2	1485	22.2		A″	32√
						1374 vw	A″	31√
31	A″	1379	0.6	1375	0.0			
30	A′	1370	9.1	1364	7.8	1335 s	A″	30√
29	A″	1370	5.5	1362	8.4		A′	29√
28	A′	1304	4.3	1300	4.7	1273 vs	A″	28√
27	A″	1292	97.2	1298	114.0		A′	27√
26	A″	1225	6.2	1222	9.5	1199 s	A″	26
25	A′	1172	6.0	1178	8.3	1155 m	A″	25√
24	A″	1145	168.3	1148	148.3	1129 vs	A′	24√
23	A′	1134	6.7	1131	5.7	1112 m	A′	23
22	A″	1102	0.0	1114	5.3	1091 w	A″	22
21	A′	1089	11.8	1082	13.3	1063 s	A′	21
20	A″	1063	0.2	1062	1.0	1045 w*	A″	20
19	A″	1037	3.0	1035	2.1	1018 w	A″	19
18	A′	1001	3.6	999	3.9	980 [c]		
17	A′	949	9.8	949	8.5	934 w	A′	18√
16	A′	936	6.1	940	7.7	927 m	A′	17√
15	A″	919	14.9	914	14.9	903	A″	16√
							A′	15√
14	A″	808	16.6	807	19.9	799 s	A″	14
							A″	13√
13	A′	788	7.3	789	7.1	782 m	A′	12√
12	A″	773	3.3	770	1.0			
11	A′	760	3.4	760	6.4	751 w	A′	11
10	A′	708	31.8	712	29.5	704 m	A′	10
9	A″	666	6.9	663	5.6	652 w	A″	9
8	A′	623	9.8	624	11.2	616 m	A′	8
7	A″	457	95.6	455	96.5	454 vs	A″	7
							A′	6√
6	A′	448	0.0	443	0.1			
5	A″	395	8.1	390	8.2	390 m	A″	5
4	A′	352	16.5	349	16.1	360 m	A′	4
3	A′	300	4.5	298	4.4	307	A′	3
2	A″	163	13.0	161	13.9	174	A″	2
1	A′	86	167.9	84	162.2	104	A′	1

[a] Frequencies, ν, in cm^{-1}; dipole strengths, D, in 10^{-40} esu^2 cm^2. [b] IR frequencies of neat liquid **2**; an asterisk denotes an inflection. vs = very strong, s = strong, m = medium, vvs = very very strong, vw = very weak, w = weak. [c] Footnote 67 of ref 3. [d] Mode assignments from ref 3 differing from those deriving from the DFT calculations are checked (√).

co-workers for the C−H stretching region of **6** and for the C−D stretching regions of **5** and **6**.[4] Their peak frequencies, ϵ and $\Delta\epsilon$ values, are also given in Tables 6 and 7. The predicted C−H stretching absorption and VCD spectra of **6** exhibit some qualitative agreement with the observed spectra (ref 4, Figure 3). Two strong absorption bands are predicted, corresponding to modes 40/41 and 42−44, with shoulders due to modes 38/39 and 45, respectively. Two strong bands are observed at 2866 and 2948 cm^{-1} and can be assigned to modes 40/41 and 42−44, respectively. Shoulders are not readily apparent. The predicted VCD spectrum (for 2*S*,6*S*-**6**) exhibits a strong positive feature due to modes 40/41 and three weaker negative features due to modes 39, 43, and 45. The experimental VCD spectrum exhibits the same sign pattern as predicted. Negative, positive, negative, and negative features are at 2868, 2890, 2938, and 2958 cm^{-1} respectively. Contrary to our prediction, however, the lowest negative VCD (2868 cm^{-1}) band coincides with the absorption peak at 2866 cm^{-1}, the positive VCD (2890 cm^{-1}) band is much higher (24 cm^{-1}) than the 2866 cm^{-1} absorption peak, the negative VCD band at 2938 cm^{-1} is lower than the absorption peak at 2948 cm^{-1}, and the negative VCD band at 2958 cm^{-1} is only 10 cm^{-1} higher. Predicted peak ϵ values are comparable to experimental values, while predicted peak $\Delta\epsilon$ values are 2−3 times larger than those observed.

The predicted C−D stretching absorption and VCD spectra are in very poor agreement with experiment for both **5** and **6**. In the case of **6**, modes 36 and 37 are predicted to be ∼60 cm^{-1} apart, leading to two absorption bands of comp-

TABLE 4: Cyclohexanone-d_6 (3)[a]

		DFT/TZ2P						
		B3LYP		B3PW91		ref 3		
mode	symmetry[b]	ν	D	ν	D	ν [c]	symmetry	mode[g]
45	A′	3099	11.2	3112	10.1	2965 vs	A′	45
44	A″	3098	20.5	3111	18.9		A″	44
43	A′	3013	27.1	3024	24.4	2900 vs	A′	43
42	A″	3006	0.9	3017	0.8		A″	42
41	A′	2275	34.4	2286	31.2	2220 s*	A′	41
40	A″	2270	15.4	2281	13.8	2209 vs	A″	40
39	A′	2265	19.8	2276	17.8	2185 s	A′	39
38	A′	2202	24.0	2210	22.5	2120 vs*	A′	38
37	A″	2200	26.1	2208	25.3	2110 vs	A″	37
36	A′	2195	24.3	2202	23.5	2096 s*	A′	36
35	A′	1776	512.6	1794	513.5	1716 vvs	A′	35
34	A′	1478	28.0	1467	31.2	1432 vs	A″	34√
33	A″	1467	26.3	1455	30.4	1424 vs	A′	33√
32	A′	1326	0.8	1318	1.8			
31	A″	1310	43.8	1310	83.8	1289 vs	A″	32√
							A′	31√
30	A″	1270	110.5	1272	91.0	1249 vs	A″	30
29	A′	1258	21.5	1253	24.1	1230 s	A′	29
28	A″	1226	8.7	1233	2.6	1211 m	A″	28
27	A′	1191	9.9	1198	6.8	1173 m	A″	27√
26	A″	1150	56.3	1153	52.9	1133 s	A′	26√
25	A″	1133	0.4	1132	0.4			
24	A′	1127	2.0	1122	2.2	1100 m	A″	25√
23	A′	1109	7.2	1100	8.3	1080 s	A′	24√
22	A″	1079	26.8	1073	22.4	1052 s	A′	23√
							A″	22
21	A′	1072	6.6	1066	7.7	1048 m*	A′	21
20	A′	997	13.4	994	14.4	977 s	A′	20
							A″	19√
19	A′	949	7.9	950	7.3	938 m	A′	18√
18	A″	933	1.6	931	0.7	918 w	A″	17√
17	A′ (A″)	907	0.2	907	7.0	897 m	A′	16√
16	A″ (A′)	901	6.7	902	0.4			
15	A″	852	31.6	853	33.8	844 vs	A″	15
14	A″	792	0.3	793	0.6	784 vw	A″	14
13	A′	758	2.9	761	1.4	754 w	A″	13√
							A′	12√
12	A″	755	8.3	751	5.9	744[d]		
11	A′	725	11.2	723	15.2	719 s	A′	11
10	A′	691	12.3	698	11.1	693 m	A′	10
9	A″	660	32.6	655	32.4	653 s	A″	9
8	A′	612	15.1	613	15.1	603 m	A′	8
7	A″	485	68.3	485	69.3	483 vs	A″	7
6	A′	429	13.5	424	14.5	435 m	A′	6
5	A″	395	18.0	390	18.1	391 m[e]	A″	5
4	A′	377	6.7	373	6.1	379 m	A′	4
3	A′	250	3.5	248	3.2	254[f]	A′	3
2	A″	159	22.7	156	24.1	164[f]	A″	2
1	A′	87	179.2	85	173.3	91[f]	A′	1

[a] Frequencies, ν, in cm^{-1}; dipole strengths, D, in 10^{-40} esu^2 cm^2. [b] B3PW91 symmetry; symmetry for B3LYP in parentheses. [c] IR frequencies of neat liquid **3**, unless indicated; an asterisk denotes an inflection. vs = very strong, s = strong, vvs = very very strong, m = medium, w = weak, vw = very weak. [d] Estimated from Figure 5C ref 3. [e] Estimated from Figure 5C ref 3; listed as 381 cm^{-1} in Table IVC, ref 3. [f] Raman frequencies. [g] Mode assignments from ref 3 differing from those deriving from the DFT calculations are checked (√).

arable intensity and two VCD bands of opposite sign with mode 36 exhibiting stronger negative VCD than the positive VCD of mode 37 for 2*S*,6*S*-**6**. Experimentally (ref 4, Figure 4), at least four bands are observed in the 2100−2250 cm^{-1} range. The VCD is negative in the region of the absorption bands at 2133 and 2160 cm^{-1} and positive in the region of the bands at 2198 and 2213 cm^{-1}. As in the C−H stretching region, VCD maxima and minima do not coincide closely with maxima in the absorption. In addition, predicted ϵ_{max} values are comparable to those observed while predicted $\Delta\epsilon_{max}$ values are nearly an order of magnitude smaller than observed values. Detailed assignment of these spectra clearly requires Fermi resonance to be taken into account.

In the case of **5**, the correspondence of theory and experiment is even worse. Two absorption features, separated by ∼60 cm^{-1}, corresponding to the two, equally populated conformations of **5** with axial and equatorial D substitution, are predicted. The VCD spectra of the two conformers is predicted to be oppositely signed for 2*R*-**5**, axial-D, and equatorial-D substitution gives positive and negative VCD bands, respectively. Experimentally, at least three features are observed in the range 2100−2250 cm^{-1} (ref 4, Figure 5). All exhibit negative VCD bands. As with **6**, the predicted ϵ_{max} values are correct in order of magnitude, while the predicted $\Delta\epsilon_{max}$ values are much smaller than observed. Again, detailed assignment is not possible.

TABLE 5: Cyclohexanone-d_{10} (4)[a]

DFT/TZ2P						ref 3		
		B3LYP		B3PW91				
mode	symmetry	ν	D	ν	D	ν [b]	symmetry	mode[e]
45	A′	2295	15.4	2305	13.6	2221 s*	A′	45
44	A″	2291	7.5	2302	6.9		A″	44
43	A′	2275	31.4	2285	28.4	2210 vs	A′	43
42	A″	2270	18.7	2281	16.9		A″	42
41	A′	2265	18.9	2276	16.8			
						2165 m	A′	41
						2125 s*	A′	40
							A″	39
40	A′	2202	25.0	2209	21.4			
39	A″	2200	24.9	2208	24.3			
38	A′	2197	21.1	2204	20.2	2111 vs	A′	38
37	A′	2194	19.0	2202	20.1		A″	37
36	A″	2190	0.5	2198	0.1			
						2083 m*	A′	36
35	A′	1771	519.4	1789	519.4	1710 vvs	A′	35
34	A″	1254	160.4	1267	169.1	1245 vs	A″	34
						1221 m	A″	33√
33	A″	1201	91.1	1216	88.9	1191 vs	A′	32
32	A′	1198	23.5	1209	24.0			
31	A′	1160	2.0	1162	1.5	1138[c]		
30	A″	1151	0.4	1157	3.9			
						1116 m	A″	31√
29	A′	1121	3.8	1116	4.0	1095 s	A′	30√
28	A′	1109	15.3	1100	18.1	1079 s	A′	29√
27	A″	1095	1.7	1087	1.9	1067 s	A′	28√
							A″	27
						1056 s	A′	26√
26	A′	1085	9.0	1076	10.7	1048 s*	A″	25√
25	A″	1074	1.1	1065	2.2	1038[c]		
24	A″	1040	22.2	1032	19.9	1016 s	A″	23√
23	A′	1022	1.7	1017	1.8	1002 m*	A′	24√
22	A′	994	4.0	991	4.2	968 m	A″	22√
21	A″	988	10.7	985	11.2			
20	A′	950	4.0	948	4.5	930 w	A′	21√
						922 w	A′	20√
19	A″	905	4.0	904	3.4	889 m	A″	19
18	A′	900	12.5	899	13.1			
						863 w	A′	18√
						827 w	A″	17√
17	A″	803	6.7	799	6.2	787 m	A″	16√
16	A′	796	5.4	796	5.2		A′	15√
15	A″	766	1.7	761	1.2			
14	A″	745	16.2	748	16.9	739 m	A″	14
13	A′	722	0.4	729	0.5	721 vw	A′	13
12	A″	704	1.2	699	2.3	682 vw	A″	12
11	A′	678	16.0	674	25.0	667 m	A′	11
10	A′	664	10.6	668	2.5	655 w*	A′	10
9	A″	625	17.2	622	15.9	612 m	A″	9
8	A′	586	16.4	587	16.6	580 m	A′	8
7	A″	453	92.8	451	94.0	450 vs	A″	7
6	A′	383	0.7	377	1.1			
5	A″	371	6.3	366	6.4	368 w	A″	6√
							A′	5√
4	A′	347	18.5	344	18.2	349 m	A′	4
3	A′	247	3.1	245	2.9	254 m[d]	A′	3
2	A″	146	16.3	144	17.4	163[d]	A″	2
1	A′	83	180.6	81	174.9	93[d]	A′	1

[a] Frequencies, ν, in cm^{-1}; dipole strengths, D, in 10^{-40} esu^2 cm^2. [b] IR frequencies of neat liquid **4**, unless indicated; an asterisk denotes an inflection. s = strong, vs = very strong, m = medium, vvs = very very strong, w = weak, vw = very weak. [c] Estimated from Figure 5D ref 3. [d] Raman frequencies. [e] Mode assignments from ref 3 differing from those deriving from the DFT calculations are checked (√).

DFT/B3LYP/TZ2P calculations for **5** and **6**, also reported in Tables 6 and 7, are in comparable agreement with experiment.

The mid-IR absorption spectra of **1** have been predicted using B3PW91 and the 6-31G* basis set and using the HF/SCF method with the TZ2P basis set. The results are compared to the B3PW91/TZ2P spectrum and to the experimental spectrum in Figure 10. Frequencies and dipole strengths are compared to experimental values in Figures 4 and 5. The B3PW91/6-31G* spectrum is qualitatively very similar to the B3PW91/TZ2P spectrum. Calculated frequencies are generally higher, as are percentage deviations from experimental frequencies. Calculated dipole strengths are in comparable agreement with experiment. The HF/SCF/TZ2P spectrum differs significantly from the B3PW91/TZ2P spectrum. Calculated frequencies are much higher, leading to percentage deviations in the range 4−14%. The intensity changes show that the HF/SCF normal coordinates

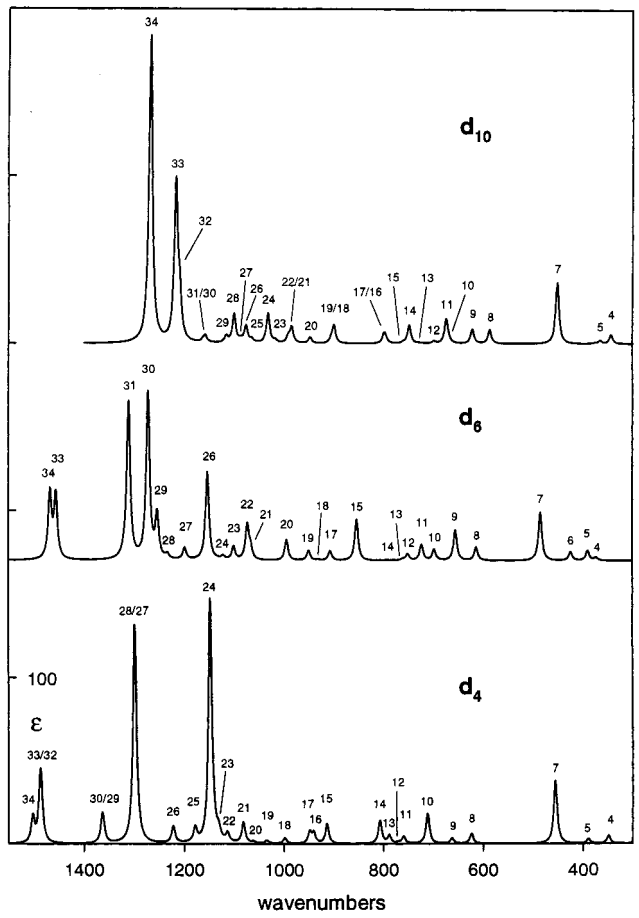

Figure 6. Calculated B3PW91/TZ2P mid-IR absorption spectra of **2**, **3**, and **4**. Lorentzian band shapes with $\gamma = 4.0$ cm^{-1} are used. Fundamentals are numbered.

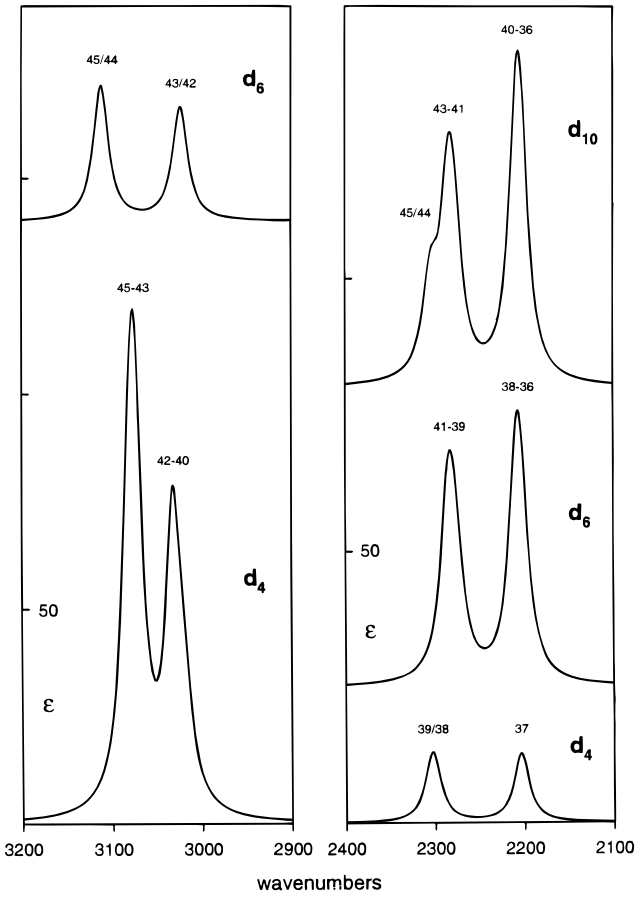

Figure 7. Calculated B3PW91/TZ2P C−H and C−D stretching absorption spectra of **2**, **3**, and **4**. Lorentzian band shapes with $\gamma = 10.0$ cm^{-1} are used. Fundamentals are numbered.

differ significantly. The pattern of intensities is in worse agreement with experiment, especially for modes 9−18 and 25−29. Calculated dipole strengths exhibit greater deviation from experimental values. The relative accuracies of the calculations are thus: B3PW91/TZ2P > B3PW91/6-31G* ≫ HF/SCF/TZ2P.

Discussion

As a result of recent developments,[16] both vibrational unpolarized absorption and circular dichroism spectra can now be efficiently predicted within the harmonic approximation using DFT. Using state-of-the-art density functionals—the Becke type "hybrid" functionals[11]—DFT is substantially more accurate than the Hartree−Fock/self-consistent field (HF/SCF) methodology. Studies of several organic molecules, including 6,8-dioxabicyclo-[3.2.1]octane and derivatives,[6,7] camphor,[8] fenchone,[8] α-pinene,[9] and phenyloxirane[10] using the B3PW91 and B3LYP functionals have documented the impressive capabilities of DFT in predicting vibrational absorption and circular dichroism spectra. In this work we extend these studies to cyclohexanone and its isotopomers. Three isotopomers, **2**−**4**, like **1** are achiral and do not exhibit VCD. Two isotopomers, **5** and **6**, are chiral and do exhibit VCD.

The mid-IR absorption spectra predicted for **1** using B3PW91 and B3LYP at the TZ2P basis set level are both in excellent agreement with experiment and lead to an identical assignment of the fundamentals of **1**. Where resolved, fundamentals are unambiguously assigned. A number of pairs of fundamentals are not resolved, and their splittings and relative intensities cannot be separately determined. In the C−H stretching region overlap is much worse and Fermi resonance with nonfundamentals is likely to be a substantial perturbation. Assignment in this region is much more complicated and is not unambiguous.

Our assignment for **1** is strongly supported by the quantitative agreement of calculated and experimental frequencies. In a prior study of 11 small molecules, DFT/B3LYP/TZ2P calculations yielded average RMS deviations of 3.2% and 1.2% from observed and harmonic frequencies respectively.[17] The deviations from observed frequencies for **1** (Figure 4) are comparable. The prior calculations demonstrated that a considerable fraction of the deviations from observed frequencies is attributable to anharmonicity; this conclusion applies equally to **1**. In addition, the agreement of calculated and experimental dipole strengths (Figure 5) is excellent, further confirming the reliability of the assignment.

In the case of isotopomers **2**−**4**, predicted B3PW91 and B3LYP/TZ2P spectra are in excellent agreement with the absorption spectra of Fuhrer et al., with the exception of C−H and C−D stretching regions, and lead to assignments of the majority of their fundamentals. The agreement of calculated and experimental mid-IR frequencies for these isotopomers is identical in order of magnitude and very similar in frequency dependence to that for **1** (Figure 4), strongly supporting the assignments. Unfortunately, experimental dipole strengths were not reported and cannot be compared quantitatively to calculated values. However, qualitative agreement of predicted and experimental intensities is excellent.

Experimental data for the chiral isotopomers **5** and **6** is limited to the C−H and C−D stretching regions. Predicted absorption

TABLE 6: Cyclohexanone-d_1 (5)[a]

Calculation (DFT/TZ2P)												
	B3LYP						B3PW91					
	ν		D		R^b		ν		D		R^b	
mode	axial	equatorial	axial	equatorial	axial	equatorial	axial	equatorial	axial	equatorial	axial	equatorial
45	3098	3098	16.4	17.7	−0.8	1.1	3112	3112	15.4	16.2	−0.7	1.0
44	3093	3067	17.8	56.1	2.4	3.2	3106	3082	16.0	51.2	2.3	3.2
43	3066	3062	51.1	35.6	−10.0	2.9	3082	3077	47.0	30.7	−8.9	4.5
42	3062	3060	36.2	50.0	14.7	1.0	3077	3074	31.4	43.1	11.1	0.1
41	3060	3025	51.5	47.1	−8.1	−4.1	3074	3036	44.6	42.9	−6.4	−11.2
40	3023	3022	39.5	25.8	0.2	−5.5	3033	3033	36.2	29.0	0.5	−2.2
39	3021	3013	22.4	5.5	−9.2	5.5	3032	3026	24.9	3.5	−8.6	9.5
38	3009	3009	17.6	15.9	2.7	−1.2	3021	3020	19.7	18.8	4.4	−2.1
37	3006	3005	6.6	2.8	0.9	−0.1	3019	3018	6.6	3.5	−0.5	0.1
36	2210	2273	9.5	8.8	4.2	−2.0	2220	2282	8.4	8.1	3.6	−1.7

Experiment[c]			
IR		VCD[b]	
ν_{max}	ϵ_{max}	ν_{max}	$\Delta\epsilon_{max} \times 10^3$
2222	2.2	2224	−1.9
2198	4.9		
		2192	−3.1
2157	2.8	2157	−1.5

[a] Frequencies, ν, in cm^{-1}; dipole strengths, D, in 10^{-40} esu^2 cm^2; rotational strengths, R, in 10^{-44} esu^2 cm^2. [b] Absolute configuration is 2R. [c] Estimated from Figure 5, ref 4.

TABLE 7: Cyclohexanone-d_2 (6)[a]

Calculation (DFT/TZ2P)						
	B3LYP			B3PW91		
mode	ν	D	R^b	ν	D	R^b
45	3093	16.6	−2.6	3106	15.3	−2.5
44	3066	53.5	6.1	3082	49.4	5.0
43	3062	34.1	−16.6	3077	29.1	−14.6
42	3060	51.3	6.8	3074	44.5	6.0
41	3024	42.4	3.4	3035	38.9	10.2
40	3022	25.3	14.2	3032	27.7	10.1
39	3012	4.7	−9.8	3025	3.4	−12.1
38	3009	15.4	2.9	3020	18.8	1.8
37	2273	8.8	2.0	2282	8.1	1.7
36	2210	9.5	−4.2	2220	8.5	−3.6

Experiment[c]			
IR		VCD[b]	
ν_{max}	ϵ_{max}	ν_{max}	$\Delta\epsilon_{max} \times 10^3$
		2958	−0.34
2948	110.9		
		2938	−0.55
		2919	0.25
		2890	2.57
2866	53.45	2868	−0.49
		2259	−2.5
2213	7.2	2224	2.7
2198	7.3	2194	3.7
		2166	−5.7
2160	4.9	2160	−5.3
2133	5.8	2130	−6.3

[a] Frequencies, ν, in cm^{-1}; dipole strengths, D, in 10^{-40} esu^2 cm^2; rotational strengths, R, in 10^{-44} esu^2 cm^2. [b] Absolute configuration is 2S,6S. [c] Taken from Table II in ref 4.

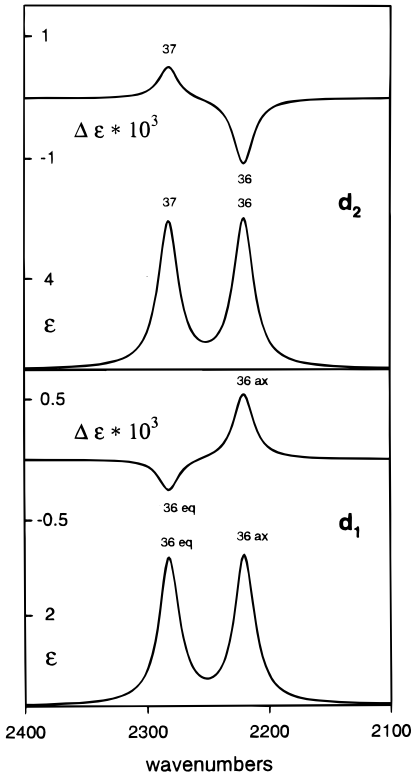

Figure 8. Calculated B3PW91/TZ2P C−D stretching absorption and VCD spectra for **5** and **6**. VCD spectra are for the (2*R*)-**5** and (2*S*,6*S*)-**6** enantiomers. Lorentzian band shapes with $\gamma = 10.0$ cm^{-1} are used. Fundamentals are numbered.

and VCD spectra are in poor agreement with experiment, as was the case for the absorption spectra of **1**−**4**. Anharmonicity and Fermi resonance are clearly responsible. Unfortunately, mid-IR spectra were not reported for these molecules and theory cannot be compared to experiment for this spectral region.

The excellent agreement of the B3PW91 and B3LYP DFT/TZ2P absorption spectra of **1**−**4** with experiment clearly shows that the harmonic potential energy surface is accurately predicted. The equilibrium geometry, corresponding to the minimum of this surface, is also accurately predicted therefore. Comparison of B3LYP TZ2P structures to experiment for a set of 11 small molecules found average RMS deviations of bond lengths and bond angles of 0.005 Å and 0.6°, respectively,[17] and this level of accuracy can be expected for the calculated structural parameters of **1**. The B3PW91 and B3LYP TZ2P

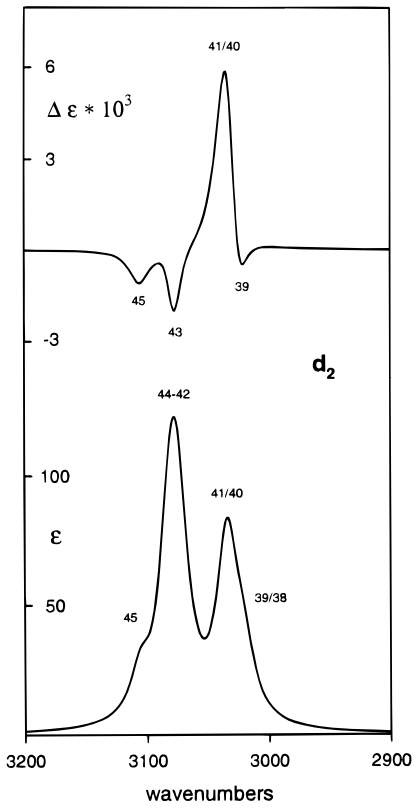

Figure 9. Calculated B3PW91/TZ2P C−H stretching absorption and VCD spectra of **6**. The VCD spectrum is for (2*S*,6*S*)-**6**. Lorentzian band shapes with $\gamma = 10.0$ cm^{-1} are used. Fundamentals are numbered.

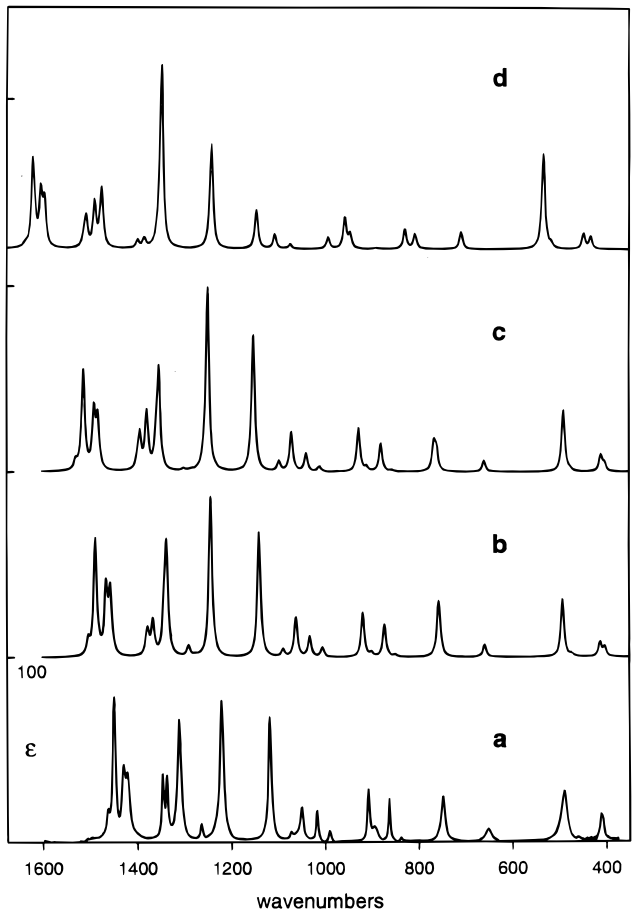

Figure 10. Mid-IR absorption spectra of **1**: (a) experimental spectrum (from Figure 2); (b−d) calculated spectra: (b) B3PW91/TZ2P, (c) B3PW91/6-31G*, (d) HF/SCF/TZ2P. Calculated spectra use Lorentzian band shapes with $\gamma = 4.0$ cm^{-1}.

structures are in quite good agreement with the experimental parameters obtained from electron diffraction data. In the cases where differences in bond lengths and angles are greater than 0.01 Å and 1°, we expect the calculated parameters to be more accurate.

The DFT calculations also provide information not available from the experimental structure. Worth noting is the variation in C−H bond lengths, all of which were assumed to be identical in the experimental structure determination. Axial and equatorial bond lengths differ significantly. The largest difference, ∼0.007 Å, is for the α C−H bonds; β and γ C−H bonds differ by 0.002−0.003 Å. The difference for the α C−H bonds is primarily due to a substantial lowering of the equatorial C−H bond length, relative to the β and γ equatorial C−H bonds. An analogous variation occurs in the bond lengths of the methyl C−H bonds of acetaldehyde and acetone: the C−H bonds coplanar with the C═O group exhibit substantially shorter bond lengths.[20]

Assignment of the fundamentals of **1**−**4** was also reported by Fuhrer et al., based on an empirical valence force field (VFF). Their assignments are given in Tables 2−5. There are many differences between our assignments and those of Fuhrer et al. It is clear that the VFF of Fuhrer et al. is substantially different from our ab initio DFT/TZ2P harmonic force fields. The reasons for this are severalfold. First, despite the large number of independent force constant matrix elements included in the refinement of the VFF, there remain many constraints. For example, stretching force constants for the C−H_{ax} and C−H_{eq} bonds are constrained to be equal. Many interaction force constants are constrained to be zero. Second, in many cases, the assignments of the observed IR absorption bands are incorrect either in regard to their symmetry or in regard to the nature of the corresponding normal coordinates. Third, as is well-known, the fitting of a VFF to a set of vibrational frequencies suffers from nonuniqueness. The detailed differences between our force fields and the VFF of Fuhrer et al. could be exposed more extensively by comparing either the force constant matrix elements or the potential energy distributions of the vibrational modes with respect to internal coordinates. At this time, this does not appear to be productive.

In the case of the C−H and C−D stretching modes of **5** and **6** assignments were attempted by Nafie and co-workers on the basis of frequencies and coordinates predicted from the VFF of Fuhrer et al. Comparison to the DFT predictions further demonstrates the major differences between the VFF and DFT force fields. For example, the VFF predicts nearly degenerate frequencies for the C−D_{ax} and C−D_{eq} stretching modes of the two conformers of **5** and of the α and α′ C−D groups of **6**. In contrast, in both molecules the DFT force fields predict differences of ∼60 cm^{-1}. The VFF assumes identical bond lengths and C−H stretching force constants for the axial and equatorial α C−H bonds of **1**. As a result the α C−D_{eq} and C−D_{ax} stretching modes of **5** and **6** are predicted to be at essentially identical frequencies. In contrast, the DFT calculations predict large (nearly 0.01 Å) differences in bond length and, consequently, substantially different stretching force constants. The α C−H_{eq} bond is shorter than the C−H_{ax}, leading to a higher force constant. As a result, the α C−D_{eq} stretching modes of **5** and **6** are predicted to be substantially higher in frequency than the α C−D_{ax} stretching modes.

The absorption and VCD spectra of the C−H and C−D stretching modes of **5** and **6** were predicted by Nafie and co-

workers using the VFF of Fuhrer et al. together with the fixed partial charge (FPC) model for vibrational electric and magnetic dipole transition moments.[21] The FPC model has since been shown to be unreliable.[22] As a result of the differences in the harmonic force field and the use of the FPC model, the absorption and VCD intensities predicted by Nafie and coworkers are quite different from those predicted by our work; any resemblance is accidental. They are also in very poor agreement with experiment.

Conclusion

We have documented the accuracy of DFT, implemented using hybrid functionals, in predicting the vibrational frequencies and unpolarized absorption intensities of the d_0, d_4, d_6, and d_{10} isotopomers of cyclohexanone. In the mid-IR, our harmonic calculations are in excellent agreement with experiment and yield essentially unambiguous assignments of the fundamental modes. Anharmonicity is a minor perturbation. For the C−H and C−D stretching modes, anharmonicity is a major perturbation and the correspondence of theory and experiment is much worse. Accordingly, without including anharmonicity, reliable assignments of the experimental spectra cannot be achieved.

When the harmonic potential energy surface is predicted accurately, it follows that the equilibrium geometry is also. The DFT geometries predicted by the B3PW91 and B3LYP functionals are very similar and in good overall agreement with the experimental structure of Dillen and Geise. The latter was not a full structure determination (i.e., a number of constraints were applied). Accordingly, given the documented accuracy of DFT in predicting molecular structures, we believe the DFT geometries to be more accurate.

We have shown that the prior vibrational analysis of **1**−**4** by Fuhrer et al. is substantially erroneous. The VFF of Fuhrer et al. has been used subsequently in analyzing the vibrational spectra of **5** and **6**. In addition, with modifications it has also been employed in analyzing the vibrational spectra of derivatives of **1**, notably 3-methyl-**1**.[23] The errors of the VFF of Fuhrer et al. lead to substantial inaccuracy in these analyses.

Our results suggest that DFT will reliably predict the structures and energies of other, higher energy conformations of cyclohexanone and also of the barriers between them and the lowest energy chair conformation. Calculations are underway to test this expectation.

Our results also lead to the conclusion that DFT calculations will permit the analysis of the vibrational spectra and conformational energetics of derivatives of cyclohexanone. The results of a study of 3-methylcyclohexanone, confirming this conclusion, will be reported in a forthcoming publication.[24]

Acknowledgment. We are grateful to NSF, NIH, and the San Diego Supercomputer Center for support of our work on vibrational spectroscopy over the years, most recently from NIH Grant R01 GM51972.

References and Notes

(1) Romers, C. *Rec. Trav. Chim. Pays-Bas* **1956**, *75*, 956.
(2) Dillen, J.; Geise, H. J. *J. Mol. Struct.* **1980**, *69*, 137.
(3) Fuhrer, H.; Kartha, V. B.; Krueger, P. J.; Mantsch, H. H.; Jones, R. N. *Chem. Rev.* **1972**, *72*, 439.
(4) Polavarapu, P. L.; Nafie, L. A.; Benner, S. A.; Morton, T. H. *J. Am. Chem. Soc.* **1981**, *103*, 5349.
(5) Laird, B. B.; Ross, R. B.; Ziegler, T. *Chemical Applications of Density Functional Theory*; ACS Symposium Series 629, American Chemical Society, Washington, DC, 1996. Seminario, J. M., Ed. *Recent Developments and Applications of Modern Density Functional Theory*; Elsevier: NY, 1996.
(6) Stephens, P. J.; Ashvar, C. S.; Devlin, F. J.; Cheeseman, J. R.; Frisch, M. J. *Mol. Phys.* **1996**, *89*, 579.
(7) Ashvar, C. S.; Devlin, F. J.; Stephens, P. J.; Bak, K. L.; Eggimann, T.; Wieser, H. *J. Phys. Chem.* **1998**, *102*, 6842.
(8) Devlin, F. J.; Stephens, P. J.; Cheeseman, J. R.; Frisch, M. J. *J. Phys. Chem.* **1997**, *101*, 6322.
(9) Devlin, F. J.; Stephens, P. J.; Cheeseman, J. R.; Frisch, M. J. *J. Phys. Chem.* **1997**, *101*, 9912.
(10) Ashvar, C. S.; Devlin, F. J.; Stephens, P. J. *J. Am. Chem. Soc.* **1998**. In press.
(11) Becke, A. D. *J. Chem. Phys.* **1993**, *98*, 1372; *J. Chem. Phys.* **1993**, *98*, 5648.
(12) Stephens, P. J.; Devlin, F. J.; Chabalowski, C. F.; Frisch, M. J. *J. Phys. Chem.* **1994**, *98*, 11623.
(13) Stephens, P. J.; Jalkanen, K. J.; Amos, R. D.; Lazzeretti, P.; Zanasi, R. *J. Phys. Chem.* **1990**, *94*, 1811.
(14) Frisch, M. J.; et al. GAUSSIAN 94 and GAUSSIAN 95 (Development Version); Gaussian, Inc.: Pittsburgh, PA.
(15) Hehre, W. J.; Schleyer, P. R.; Radom, L.; Pople, J. A. *Ab Initio Molecular Orbital Theory*; Wiley: New York, 1986.
(16) Johnson, B. G.; Frisch, M. J. *Chem. Phys. Lett.* **1993**, *216*, 133; *J. Chem. Phys.* **1994**, *100*, 7429. Cheeseman, J. R.; Frisch, M. J.; Devlin, F. J.; Stephens, P. J. *Chem. Phys. Lett.* **1996**, *252*, 211.
(17) Finley, J. W.; Stephens, P. J. *J. Mol. Struct.* (*THEOCHEM*) **1995**, *357*, 225.
(18) Carreira, L. A.; Lord, R. C. *J. Chem. Phys.* **1969**, *51*, 3225.
(19) Smithson, T. L.; Ibrahim, N.; Wieser, H. *Can. J. Chem.* **1983**, *61*, 1924.
(20) Devlin, F. J.; Stephens, P. J. Unpublished calculations.
(21) Schellman, J. A. *J. Chem. Phys.* **1973**, *58*, 2882; *J. Chem. Phys.* **1974**, *60*, 343.
(22) Stephens, P. J.; Jalkanen, K. J.; Kawiecki, R. *J. Am. Chem. Soc.* **1990**, *112*, 6518.
(23) For example, see: Polavarapu, P. L.; Nafie, L. A. *J. Chem. Phys.* **1980**, *73*, 1567. Marcott, C.; Scanlon, K.; Overend, J.; Moscowitz, A. *J. Am. Chem. Soc.* **1981**, *103*, 483. Freedman, T. B.; Kallmerten, J.; Lipp, E. D.; Young, D. A.; Nafie, L. A. *J. Am. Chem. Soc.* **1988**, *110*, 689.
(24) Devlin, F. J.; Stephens, P. J. To be published.